

TILTING SATURN

I. ANALYTIC MODEL

William R. Ward

Southwest Research Institute

1025 Walnut St. Suite 400, Boulder, CO 80302

and

Douglas P. Hamilton

Department of Astronomy, University of Maryland

College Park, Maryland

Abstract. The tilt of Saturn's spin axis to its orbit plane is 26.7° , while that of Jupiter is only 3.1° . We offer an explanation for this puzzling difference owing to gravitational perturbations of Saturn by the planet Neptune. A similarity between the precession period of Saturn's spin axis and the 1.87×10^6 year precession period of Neptune's slightly inclined orbit plane implicates a resonant interaction between these planets as responsible for tilting Saturn from an initially more upright state. We make a case that Saturn was captured into this resonance during the erosion of the Kuiper belt, which decreased the rate of regression of Neptune's orbit plane. Penetrating the resonance pumped up Saturn's obliquity to its current value. The spin axis may also be librating in the resonance with an amplitude $\psi \gtrsim 31^\circ$, and we discuss possible causes of this and the implied constraint on the Saturn moment of inertia. Matching the current pole position to the predicted outcome could place constraints on early solar system processes.

Submitted to *Astronomical Journal* December, 2003

Revised June, 2004

I. INTRODUCTION

Jupiter and Saturn consist predominantly of hydrogen and helium acquired from the primordial solar nebula during the planet building epoch. The formation of such gas giants is believed to commence with the collisional accretion of a several earth mass core from solid ice + rock planetesimals followed by the accretion of the gaseous component once the core reaches a critical size (*e.g.*, Pollack *et al.* 1976; Wuchterl *et al.* 2000 and reference therein). Seemingly at odds with this picture, however, are the very dissimilar obliquities, θ , of these planets to their orbit planes, *viz.*, 26.7° for Saturn vs. only 3.1° for Jupiter.

The obliquities of the other planets in the solar system are likely due to the stochastic nature of their accumulation from solid planetesimals (Lissauer and Safronov 1991, Dones and Tremaine 1993; Chambers 1998; Agnor *et al.* 1999), and the rock/ice cores of Jupiter and Saturn probably had non-zero obliquities as well. However, their massive gas component derived from the nebula disk would have added angular momentum nearly perpendicular to their orbit planes, overwhelming that of the cores, and ultimately resulting in small obliquities for both planets. With 95 earth masses and a 10.7 hr rotation period, Saturn has considerable spin angular momentum, making it problematic that an impact could have sufficiently changed its pole direction after its formation. Why then is Saturn's obliquity so large?

We suggest the answer lies in solar system events following the formation of the planets that caused an initially upright Saturn to suffer a tilt. We are not the first to seek such a mechanism. It has been proposed that the obliquities of the outer planets may result from a 'twist' of the total angular momentum of the solar system during the collapse of the molecular cloud core that led to its formation (Tremaine 1991). It is possible to choose a time scale for this event that would affect the planetary obliquities from Saturn on out, but have only a minor influence on Jupiter. Although this cannot be ruled out, this paper presents what we believe is a more compelling mechanism for generating Saturn's obliquity predicated on a similarity between Saturn's spin axis precession period and the regression period of Neptune's orbit plane (Harris and Ward, 1982), which seems too close to be a coincidence. We propose that this period match and the obliquity of Saturn are cause and effect through the operation of a secular spin-orbit resonance between these bodies. This type of interaction is

already known to cause large-scale oscillations of the obliquity of Mars (Ward 1973, 1974, 1979; Lascar and Robutel 1993; Touma and Wisdom 1993). Here and in a companion paper (Hamilton and Ward 2004; hereafter paper II) we detail how this mechanism could also account for the spin axis orientation of Saturn, as well as provide a sensitive constraint on its moment of inertia.

II. PRECESSIONAL MOTIONS

a. Spin Axis

The equation of motion for a planet's unit spin axis vector, \mathbf{s} , is $d\mathbf{s}/dt = \boldsymbol{\alpha}(\mathbf{s}\cdot\mathbf{n})(\mathbf{s}\times\mathbf{n})$ where \mathbf{n} is the unit vector normal to the planet's orbit plane. The precessional constant depends on the strength of the torque exerted on the planet and its spin angular momentum. For Saturn, most of the solar torque is exerted on its satellites instead of directly on the planet, Titan ($M_{Titan} = 1.34 \times 10^{26} \text{ g}$) being by far the dominant one (Ward 1975). Saturn's oblate figure gravitationally locks the satellites to its equator plane so that the system precesses as a unit (Goldreich 1965). The precessional constant can be written (Ward 1975; French *et al.* 1993)

$$\boldsymbol{\alpha} = \frac{3}{2} \frac{n^2}{\omega} \left(\frac{J_2 + q}{\lambda + \ell} \right) \quad (1)$$

where ω is the spin frequency of Saturn, n is its heliocentric mean motion, $J_2 = 1.6297 \times 10^{-2}$ is the coefficient of the quadrupole moment of its gravity field, λ is the moment of inertia, I , of Saturn normalized to $M_s R^2$, with M_s and R being the mass and radius of the planet. The quantity

$$q \equiv (1/2) \sum_j (m_j/M_s) (\alpha_j/R)^2 \sin(\theta - i_j) / \sin\theta \quad (2)$$

is effective quadrupole coefficient of the satellite system with q/J_2 being the ratio of the solar torque on the satellites to that directly exerted on the planet, and

$$\ell \equiv \sum_j (m_j/M_s)(a_j/R)^2(n_j/\omega) \quad (3)$$

is angular momentum of the satellite system normalized to $M_s R^2 \omega$, where M_j , a_j , and n_j are the masses, orbital radii and mean motions of its satellites, with i_j being the inclination of a satellite orbit to the equator of Saturn.¹ French *et al.* (1993) give $q=0.05164$ and $\ell = 0.00278$; Hubbard and Marley (1989) find $\lambda = 0.2199$ from their interior models, but this value is uncertain by as much as 10% (French *et al.* 1993; Marley personal communication). With these numbers, equation (1) yields $\alpha = 0.8306''/\text{yr}$, $\alpha \cos\theta = 0.7427''/\text{yr}$. If the orbit plane of Saturn were fixed in inertial space, its spin axis precession would occur at constant obliquity θ with a period $P = 2\pi/\alpha \cos\theta = 1.745 \times 10^6$ years.

Nicholson and French (1997) have analyzed 22 reported ring plane crossings spanning a period of 280 years to estimate Saturn's pole precession frequency as $0.51 \pm 0.14''/\text{yr}$, but this is low largely because of a ~ 700 year modulation due to Titan's 0.32° proper inclination (Nicholson *et al.* 1999). Using the nutation model of Vienne and Duriez (1992), the current rate can be predicted to be 68% of the long term value, implying $\alpha \cos\theta = 0.75 \pm 0.21''/\text{yr}$.

b. Orbit Plane

All of the planetary orbits have small inclinations to the invariable plane and undergo non-uniform regressions due to their mutual gravitational perturbations. The inclination I and ascending node Ω of a given planet is then found from a superposition (*e.g.*, Brouwer and vonWoerkom 1950; Bretagnon 1974; Applegate, *et al.* 1986; Bretagnon and Francou 1992),

$$\sin(I/2)\sin\Omega = \sum_j (I_j/2)\sin(g_j t + \delta_j) \quad ; \quad \sin(I/2)\cos\Omega = \sum_j (I_j/2)\cos(g_j t + \delta_j) \quad (4)$$

comprised of many terms of amplitudes $\{I_j\}$ and frequencies $\{g_j\}$. Nevertheless, most of them are of only minor importance, and the largest amplitude terms for Saturn's orbit are listed in Table 1; they represent contributions from three of the eight fundamental modes of a Laplace-

¹The Laplace plane at the distance of Iapetus is inclined by 14.8° to Saturn's equator, and Iapetus precesses about its normal in $\sim 3 \times 10^3$ years. Thus its average i is 14.8° as well.

Lagrange solution of the secular evolution of the solar system as given by Bretagnon (1974). The first of these is due to a strong 4.92×10^4 year mutual orbital precession of Jupiter and Saturn, the next two are perturbations to Saturn's orbit plane due to the nodal regressions of Uranus (4.33×10^5 years) and Neptune (1.87×10^6 years), respectively.

TABLE 1: Largest Amplitude Terms for Saturn's Orbit

j	$g_j (" yr^{-1})$	$I_j (^\circ)$
16	-26.34	0.910
17	- 2.99	0.045
18	- 0.692	0.064

The variations in inclination and precession rate of the orbit cause a complicated time dependence for the orbit normal $\mathbf{n}(t)$ in the equation of motion for \mathbf{s} . This can lead to oscillations of the planet's obliquity as the spin axis attempts to precession about the moving orbit normal. In a linearized solution (*e.g.* Ward 1974; eqn. (5) below) conspicuous oscillations occur because there is a near match between the spin axis precession rate $\alpha \cos \theta$ and $-g_{18}$, but again, the relative closeness of these frequencies for Saturn is due in part to its current obliquity. On the other hand, there are very good reasons to believe that both α and g_{18} were different in the past. For example, the spin axis precession rate would have varied during the early contraction of Saturn as its cooled soon after formation (Pollack, *et al.* 1976; Bodenheimer and Pollack 1986), while the frequency g_{18} would have been faster in early solar system due to the presence of a larger population of objects in the Kuiper belt (Holman and Wisdom 1993; Duncan, *et al.* 1995; Malhotra, *et al.* 2000) whose gravitational influence would have increased Neptune's regression rate. Thus, if the similar values of $\alpha \cos \theta$ and $-g_{18}$ are not coincidental, something must have maintained this relationship during these changes. The current paper applies the theory of secular spin-orbit resonance to the Saturn/Neptune interaction, and demonstrates the ability of the resonance to drive up Saturn's obliquity from

an initially near zero value. Our companion paper presents numerical experiments that further support the efficacy of this mechanism.

III. SECULAR SPIN-ORBIT RESONANCE

a. Spin Axis Trajectories

Since there are many terms in equation (4), neither the inclination nor the regression rate $\dot{\Omega}$ of the orbit are constant. In the case of small angles, the equation of motion for the spin axis can be linearized and solved analytically to give an expression for obliquity variations of the form (Ward 1974)

$$\theta \approx \bar{\theta} - \sum_j \left(\frac{g_j I_j}{\alpha \cos \bar{\theta} + g_j} \right) \sin(\alpha t \cos \bar{\theta} + g_j t + \Delta_j) \quad (5)$$

where $\bar{\theta}$ is a long-term average obliquity and the $\{\Delta_j\}$ are phase constants that depend on the observed planetary orbits. In general, the various sinusoidal terms cause rapid oscillations compared to any change in $\bar{\theta}$. However, if for some $j = J$, $\alpha \cos \bar{\theta} \rightarrow -g_j$, that term's small denominator causes its amplitude to become very large while its frequency becomes very slow. The combination of this J -term plus $\bar{\theta}$ can then be replaced by a slowly moving non-linear guiding center $\theta_{gc}(t)$ about which the other terms cause a high frequency circulation of the spin axis (Ward 1992). It turns out that the high frequency terms do not interfere much with the motion of the guiding center even if $\alpha \cos \theta_{gc}$ passes through $-g_j$, although in this case the linearized version of $\theta_{gc}(t)$ is no longer valid. One can show both analytically (Ward *et al.* 1979) and numerically (Ward 1992; paper II) that the motion of the guiding center is quite similar to the spin axis motion in the case of uniform orbital precession provided we set $I = I_J$, $\dot{\Omega} = g_J$. We turn to that case now.

Consider an orbital precession obtained by retaining only a single term J in the precession equation (4). In this case, \mathbf{n} maintains a constant inclination $I = I_J$ to the fixed normal to the invariable plane \mathbf{k} , and precesses at a constant rate $\dot{\Omega} = g_J = \mathbf{g}$ (Figure 1). If a coordinate frame rotating with angular frequency \mathbf{g} is adopted, the orbit normal \mathbf{n} will

appear fixed. The equation of motion for the unit spin vector of a planet now takes the form

$$ds/dt = \alpha(\mathbf{s} \cdot \mathbf{n})(\mathbf{s} \times \mathbf{n}) + \mathbf{g}(\mathbf{s} \times \mathbf{k}) \quad (6)$$

This problem is well studied (*e.g.*, Colombo 1966; Peale 1969, 1974; Ward *et al.* 1979; Henrard and Murigande 1987), and an exact integral of the motion can be found, which is also the relevant portion of the Hamiltonian of the system, $H = -(\alpha/2)(\mathbf{n} \cdot \mathbf{s})^2 - \mathbf{g}(\mathbf{k} \cdot \mathbf{s})$ (*e.g.*, Ward 1975). In the next section we use H together with the elegant Cassini state theory as developed by Colombo, Peale and others.

b. Cassini States

Colombo (1966) showed that the unit spin axis $\mathbf{s} \equiv (x, y, z) = (\sin \theta \cos \phi, \sin \theta \sin \phi, \cos \theta)$ traces out a closed curve on the unit sphere, $x^2 + y^2 + z^2 = 1$, given by its intersection with a cylindrical parabola,

$$[z + (g/\alpha)\cos I]^2 = -2(g/\alpha)\sin I(y - K) \quad (7)$$

as shown in Figure 2. This describes a family of parabolae with latus rectum $p = -(g/\alpha)\sin I$ and axis $z_o = -(g/\alpha)\cos I$ but various vertices K . Depending on the choice of g/α and the resulting location of the axis z_o , there are either two or four locations (called Cassini states and denoted by the vectors $s_1 \rightarrow s_4$ in Figure 2) where a parabola is tangent to the unit sphere for some value of the vertex and the trajectory degenerates to a point. Here the spin axis \mathbf{s} remains co-planar with \mathbf{n} and \mathbf{k} and stationary in the rotating frame, which means that in inertial space, these vectors co-precess at the same rate g , as depicted in Figure 1. Two of the states (labeled 1 and 4) are on the same side of \mathbf{k} as \mathbf{n} , while state 2 is on the opposite side (Cassini state 3, which is retrograde, will not further concern us here). If the convention introduced by Peale (1974) of measuring θ_i clockwise from \mathbf{n} is used, the state obliquities can be found from the single relationship,

$$(\alpha/g)\cos\theta_i \sin\theta_i + \sin(\theta_i - I) = 0 \quad (8)$$

obtained by setting $\dot{\theta}, \dot{\phi} = 0$ in eqn. (6). This is equivalent to a quartic equation which could be solved explicitly for its four roots. Figure 3 shows a plot of the Cassini state obliquities $\theta_1, \theta_2, \theta_4$ as functions of α/g where a value of $I = I_{18}$ has been adopted. It can be seen that for $|\alpha/g|$ less than some critical value, states 1 and 4 do not exist. This value can be determined by differentiating eqn (8) and setting $d\theta/d(\alpha/g) = \infty$ at $(\alpha/g)_{crit}$ to find the condition $(\alpha/g)_{crit} \cos 2\theta + \cos(\theta - I) = 0$. Combining with eqn (8), one can solve for the critical values of $\theta_1 = \theta_4 = \theta_{crit}$ and $(\alpha/g)_{crit}$, viz.,

$$\tan \theta_{crit} = -\tan^{1/3} I \quad ; \quad (\alpha/g)_{crit} = -(\sin^{2/3} I + \cos^{2/3} I)^{3/2} \quad (9)$$

For I_{18} , $\theta_{crit} = -5.92^\circ$ and $(\alpha/g)_{crit} = -1.016$.

Rearranging eqn. (8) into the form $[(\alpha/g)\cos\theta + \cos I]\tan\theta = \sin I \ll 1$, it is clear that the LHS can be made small by either a small value of $\tan\theta$ for which $\cos\theta \sim O(\pm 1)$, or by making the bracketed term small. These conditions yield the following approximate formulas,

$$\theta \approx \tan^{-1}[\sin I / (1 \pm \alpha/g)] \quad ; \quad \theta \approx \pm \cos^{-1}[-g \cos I / \alpha] \quad (10)$$

When $|\alpha/g| > |\alpha/g|_{crit}$, the first expression approximates states 1 and 3 corresponding to $\pm\alpha$, respectively, while the second gives states 2 and 4. When $|\alpha/g| < |\alpha/g|_{crit}$, the first expression gives states 2 and 3, while the bracketed quantity cannot approach zero and the two corresponding roots of the quartic equation are complex. In this case, states 1 and 4 do not exist. States 1 through 3 are stable in the sense that if the spin axis is slightly displaced from them, it will tend to circulate the state; state 4 is unstable in this regard and lies on a separatrix (Figure 2b), which partitions the unit sphere into three domains, each containing a stable state.

c. Spin Axis Position

To evaluate whether Saturn could be in the resonance, its spin axis must be located with respect to the $j = 18$ reference frame defined by a z -axis that lies along the pole of the term, and an x -axis along its ascending node on the invariable plane of the solar system. The right ascension and declination of s with respect to the equator and equinox at epoch J2000.0

are 40.595° and 83.537° respectively (Yoder 1995). Rotating about the vernal equinox by the Earth's obliquity, 23.439° (Yoder 1995), gives \mathbf{s} with respect to the ecliptic and equinox as

TABLE II:
Coordinates of Saturn Spin Axis, $j = 18$ Pole, and Normal to Invariable Plane

Vector	Reference frame	i	Co-latitude*	Longitude	x	y
\mathbf{s}	Ecliptic/equinox		28.049°	79.509°	8.546×10^{-2}	4.624×10^{-1}
\mathbf{k}	“		1.579°	17.582°	2.627×10^{-2}	8.322×10^{-3}
\mathbf{k}	Invariable plane		0	---	0	0
\mathbf{s}	“		27.254°	68.491°	5.919×10^{-2}	4.541×10^{-1}
\mathbf{n}	“		0.0644°	66.476°	4.488×10^{-4}	-1.031×10^{-3}
\mathbf{k}	Intermediate		0.0644°	113.523°	-4.488×10^{-4}	1.031×10^{-3}
\mathbf{s}	“		27.315°	82.264°	5.874×10^{-2}	4.551×10^{-1}
\mathbf{n}	“		0	---	0	0
\mathbf{k}	$j = 18$ system		0.0644°	90°	0	1.124×10^{-3}
\mathbf{s}	“		27.315°	59.122°	2.355×10^{-1}	3.938×10^{-1}
\mathbf{n}	“		0	---	0	0

* For \mathbf{s} , the co-latitude is the obliquity, for \mathbf{k} , \mathbf{n} it is the inclination

shown in Table II. The normal \mathbf{k} to the invariable plane from Allen is listed as well. Also included in the table are the x and y components of each vector in each system. Since the inclination of the invariable plane is very small, to first order accuracy the coordinate system can be transformed to that plane by subtracting the components of \mathbf{k} from \mathbf{s} . We now introduce the $j = 18$ pole from Applegate *et al.* (1986), who give² $\{p, q\} = \sin(I_{18}/2)\{\sin, \cos\}\Omega_{18} = N_8\{\sin, \cos\}\delta_8$, where $N_8 = -10^{-3.25}$, $\delta_8 = 203.518^\circ$. Setting $\sin(I_{18}/2) \approx (1/2)\sin I_{18}$, and recalling that the longitude of the pole is 90° behind its ascending node Ω_{18} , we find the components of \mathbf{n} listed in Table II. We can transform again to a system with \mathbf{n} at origin by subtracting its components from the other vectors. This gives

¹ In the Applegate *et al.* (1986) notation, our $j=18$ is their $j = 8$.

the vectors in an intermediate system. A final counter-clockwise rotation of the coordinate system by 23.523° puts k in the y -axis. The spin axis lies $\psi = 90^\circ - 59.1^\circ = 30.9^\circ$ from k . Figure 4 shows polar views of the $j = 18$ system for $\alpha/g_{18} = -1.16$ along with the separatrix, and $s = (x_s, y_s, x_s) = (0.236, 0.394, 0.888)$. The separatrix is more narrow than the example of Figure 2 because the inclination is an order of magnitude smaller. Since the trajectory does not enclose n at the origin, such motion produces the longitude libration diagnostic of resonance trapping.

d. System Evolution

If the frequency ratio α/g changes for some reason, the Cassini states migrate along the unit sphere in accordance equation (8) and Figure 3. If changes occur slowly enough, it can be shown that the area enclosed by the spin axis trajectory about the local Cassini state remains nearly invariant (*e.g.*, Peale 1974; Ward *et al.* 1979). Slowly enough means that the state migration rate is much less than the rate of spin axis motion: the so-called adiabatic limit. In particular, if the spin axis starts near state 2 with $|\alpha/g| \ll 1$, it will remain so as $|\alpha/g|$ increases and the state migrates away from n (at $\theta = 0$). As the frequency ratio passes through the critical value, the obliquity rises steeply and can become quite large; this is resonance *capture*.

By contrast, with $|\alpha/g| \gg 1$, state 1 is near n , but rotates away as $|\alpha/g|$ decreases, while state 4 rotates toward it. The two states eventually merge at $(\alpha/g)_{crit}$; past this, state 2 is the only prograde state. A spin axis initially close to state 1 will track its motion until its merger with state 4. At this point it is left stranded and must establish a new trajectory about state 2, enclosing an area that may no longer be small. This sequence is resonance passage in the *non-capture* direction and results in a ‘kick’ to the obliquity. Consequently, passage through the resonance is not a reversible process, with the outcome depending on direction. Employing elegant analytical expressions derived by Henrard and Murigande (1987) for the areas inside each of the domains, the above arguments are easily quantified. The area inside the separatrix containing state 2 can be written as,

$$A_2 = 8\rho + 4\tan^{-1}T - 8z_o \tan^{-1}(1/\chi), \quad (11)$$

where

$$\chi \equiv \sqrt{-\tan^3\theta_4/\tan I - 1}, \quad (12)$$

which starts at $\chi = 0$ for $\theta_4 = \theta_{crit}$, and diverges as $\theta_4 \rightarrow -\pi/2$. The remaining functions can be written

$$\rho \equiv \frac{\chi \sin^2\theta_4 \cos\theta_4}{\chi^2 \cos^2\theta_4 + 1} \quad ; \quad T \equiv \frac{2\chi \cos\theta_4}{\chi^2 \cos^2\theta_4 - 1} \quad (13)$$

where the second quadrant value of $\tan^{-1}T$ is to be used when $T < 0$. The other two domain areas can now be written in terms of eqn. (11),

$$A_{1(3)} = 2\pi[1 - (+)z_o] - A_2/2 \quad (14)$$

Figure 6 displays the domain areas as a function of $\alpha/g = \sin I/\sin\theta_4 - \cos I/\cos\theta_4$. Note that when $\chi = 0$; $\rho = 0$, $\tan^{-1} T = \pi$, $\tan^{-1}(1/\chi) = \pi/2$. Substituting these values into eqn (11) yields the critical value of $A_2 = A_{crit} = 4\pi(1 - z_{crit})$ for which A_1 vanishes, indicating the merger of states 1 and 4. Finally, setting $z_{crit} = -(g/\alpha)_{crit} \cos I$, the area surrounding state 2 at merger becomes

$$A_{crit} = 4\pi[1 - (1 + \tan^{2/3}I)^{-3/2}] \quad (15)$$

If state 2 were to then migrate near the orbit normal (*i.e.*, $|\alpha/g| \ll 1$), the precession would become almost uniform with an obliquity given by

$$\cos\theta = 1 - A_{crit}/2\pi = \frac{2}{(1 + \tan^{2/3}I)^{3/2}} - 1 \quad (16)$$

Figure 5 shows this obliquity as a function of inclination amplitude. Again, these are adiabatic values corresponding to arbitrarily slow passage. The obliquities for amplitudes in

Table I are indicated on the curve; for $I_{18} = 0.064^\circ$, $\theta = 14.5^\circ$.

IV. TUNING MECHANISMS

If Saturn was captured into a secular spin-orbit resonance with Neptune, how and when did this occur? For the present frequency ratio, state 1 lies very close to the pole position of the $j = 18$ term (Figure 4). It is only because of Saturn's large obliquity that the ratio of Neptune's orbit precession rate to Saturn's pole precession rate could be near unity. To account for this as a result of resonance capture, the case must be made for either an increase in α and/or a decrease in $|g_{18}|$ to 'tune' the system through the critical frequency ratio in the proper direction. Below we discuss possible adjustments in the early solar system that could account for this, although they may not be unique.

a. The Kuiper Belt.

Neptune's nodal line regression is caused by the orbit averaged gravity of the planets interior to it. If there were planets exterior to Neptune they would each contribute to g_{18} by an amount

$$\delta g \approx -\frac{n_N}{4} \left(\frac{M_p}{M_\odot}\right) \left(\frac{a_N}{a_p}\right)^2 b_{3/2}^{(1)}(a_N/a_p) \quad (17)$$

where M_p , a_p are the planet's mass and semimajor axis, $a_N = 30.1 AU$, $n_N = 7.85 \times 10^3 \text{ ''/yr}$ are the semimajor axis and mean motion of Neptune, M_\odot is the solar mass, and the quantity $b_{3/2}^{(1)}(\gamma)$ is a Laplace coefficient (*e.g.*, Brouwer and Clemence 1961). Pluto does this, but its mass is so small ($M_p = 2.2 \times 10^{-3} M_{Earth}$, $a_p = 39.5 AU$) that its fractional contribution is only $\delta g/g_{18} \approx 3 \times 10^{-5}$. However, Pluto is generally regarded as a remnant of a larger Kuiper belt population that was eroded away over time (*e.g.*, Holman and Wisdom 1993; Duncan *et al.* 1995). The contribution of a primordial Kuiper Belt of surface density σ to Neptune's precession can be estimated by replacing M_p by $2\pi\sigma r dr$ in eqn. (17) and integrating over the width of the belt. Starting at Pluto's distance, $r_K \sim 40 AU$, and integrating to $\sim 50 AU$ where recent observations indicate an outer edge to the belt (Allen *et al.* 2001; Trujillo and

Brown 2001) yields a fractional contribution of order $\delta g/g_{18} \approx 10^{-2}(M_K/M_{Earth})$, or about 1% for each earth mass of material. The present mass M_K of the Kuiper Belt is of order $few \times 10^{-1}M_{\oplus}$, but its primordial mass, estimated by extrapolating the planetesimal disk from Neptune into the region, could have been as high as $few \times 10M_{\oplus}$ (e.g., Stern and Colwell 1997; Farinella *et al.* 2000; Malhotra *et al.* 2000). This is sufficient to place Saturn to the left of $(\alpha/g)_{crit}$ in Figure 3, implying that it passed through the resonance in the capture direction as the mass of the belt diminished. We should also point out that a concomitant outward migration of Neptune (e.g., Hahn and Malhotra 1999) would result in a decreasing $|g_{18}|$ as well. Numerical experiments of the erosion of the belt indicate a time scale in excess of $O(10^8)$ years for the portion of the belt beyond $\sim 40 AU$. The final obliquity of Saturn would then simply be the limiting value it acquired by the time the Kuiper Belt mass was exhausted.

b. Spin Axis Librations.

If Saturn is currently trapped in the resonance, Figure 4 shows that it is librating about state 2. The inferred libration amplitude ψ_{max} is sensitive to where we put the separatrix or equivalently to the exact value of α/g_{18} . There is some uncertainty in g_{18} , but it is probably small; the planetary theory constructed Bretagnon (1994) including fourth-order long-period terms with short-period term corrections gives $0.691'' yr^{-1}$, while Applegate *et al* (1986) Fourier transform the orbital elements of a 100 Myr numerical integration of the outer five planets to find $0.692'' yr^{-1}$. The greatest uncertainty in α is thorough the moment of inertia of Saturn, but resonance occupancy places a constraint on λ .

The smallest area enclosed by a librating trajectory is found by making the current spin axis position the amplitude ψ_{max} , while the largest area is found by putting Saturn's pole on the separatrix itself, for z_o either greater or less than z_s so that $\psi_{max} = \pi$. The area inside the current trajectory can be found as a function of α/g ,

$$A = \int_{traj} \sin\theta d\theta d\phi = \int dz d\phi = \int_{z_1}^{z_2} [\pi/2 - \phi(z)] dz \quad (18)$$

where $\sin\phi(z) = [K + (z - z_o)^2/2p]/(1 - z^2)^{1/2}$ and the integration limits are the values of z for

which $\sin \phi(z) = 1$ (Ward *et al.* 1979). Saturn's current pole position constrains allowable values for the vertex, $K = y_s + (z_s - z_o)^2/2p$. The minimum $K_{\min} = y_s$ occurs when $z_o = z_s$ and $\alpha/g_{18} = -\cos I/z_s = -1.126$. The associated value of $A = 0.0167$ sets a minimum pre-capture obliquity of $\theta_{\min} = 4.2^\circ$. A curve of A values compatible with the current s is included in Figure 6. The inferred range of uncertainty in the frequency ratio, $1.078 < |\alpha/g| < 1.182$, can be related to Saturn's moment of inertia through equation (1), *i.e.*, $0.2233 < \lambda < 0.2452$ gives the range of values for which Saturn could be currently trapped in the resonance. The minimum is $\sim 1\%$ larger than the Hubbard and Marley value but well within its uncertainty.

For I_{18} , $A_{crit} = 4\pi(1 - z_{crit}) = 0.2003$; projecting this case back to $|\alpha/g| \ll |\alpha/g|_{crit}$, gives the maximum obliquity, $\theta = \cos^{-1}[2z_{crit} - 1]$, for certain capture, which turns out to recover equation (16), *i.e.*, $\theta = 14.5^\circ$. From Figure 6, $A = A_{crit}$ for $\alpha/g_{18} = -1.084$ and -1.169 . The corresponding inertia range is $0.2257 < \lambda < 0.2438$. Capture is possible for larger θ , but at a decreasing probability given by

$$P = |\dot{A}_2/\dot{A}_3| = 2/(1 - 4\pi\dot{z}_o/\dot{A}_2) \quad (19)$$

The rate of change of A_2 is found from $\dot{A}_2 = \dot{z}_o \partial A_2 / \partial z_o + \dot{p} \partial A_2 / \partial p$, where the partial derivatives are given by Henrard and Murigande (1987)

$$\partial A_2 / \partial z_o = -8 \tan^{-1}(1/\chi) \quad ; \quad \partial A_2 / \partial p = 8\rho/p \quad (20)$$

Substitution into eqn. (19) yields

$$P = \frac{2}{1 + \frac{\pi}{2} [\tan^{-1}(1/\chi) - \rho/z_o]^{-1}} \quad (21)$$

which is to be evaluated at the moment of separatrix crossing. If, when $|\alpha/g| \ll |\alpha/g|_{crit}$, the original obliquity is $\theta_o > 14.5^\circ$, the area $A_o = 2\pi(1 + \cos \theta_o)$ of the unit sphere below the

trajectory is less than value of A_3 when the separatrix first appears, *i.e.*, the spin axis is in domain 3 outside of the separatrix. As $|\alpha/g|$ increases, both A_1 and A_2 increase at the expense of A_3 as shown in Figure 6. The spin axis crosses the separatrix when $A_o = A_3$, or $A_2 = 4\pi(z_o - \cos\theta_o)$. Combining with eqn. (11) this condition reads,

$$z_o[1 + \frac{2}{\pi}\tan^{-1}(1/\chi)] - \frac{1}{\pi}(2\rho + \tan^{-1}T) = \cos\theta_o \quad (22)$$

which can be used to determine the transition values of χ and θ_4 . Using these in eqn. (21) yields the probability. Figure 7 shows the capture probabilities as a function of the pre-capture obliquity.

V. DISCUSSION

What would be a likely origin of Saturn's libration? One clear possibility is a late impact. A fortuitous grazing impact near Saturn's pole at its escape velocity will shift the spin axis by $\delta\theta \sim (m/\lambda M)(GM/\omega^2 R^3)^{1/2} \sim 7^\circ(m/M_\oplus)$, where m and M_\oplus are masses of the projectile and the Earth, respectively; more probable impact parameters and angles would require several earth masses. On the other hand, if the impact post-dated resonance capture, the elongated nature of the trajectories decreases the required obliquity change by a factor $(\tan I/\tan\theta_o)^{1/4} \approx 0.22$ (see paper II). Indeed if the impactor shifts the axis more than the half-width of the separatrix itself, $\Delta\theta_s = 2\sqrt{\tan I/\tan\theta_o} = 5.4^\circ$, it would knock Saturn out of the resonance. Another way to generate libration is by a somewhat non-adiabatic passage through the $j = 18$ resonance in the capture direction on a time scale comparable to the libration time of $\sim 8 \times 10^7$ years. We note this is not too different from the erosion timescale of the Kuiper belt, and numerically assess this possibility in our companion paper II. Non-adiabaticity may also be introduced if Neptune migrates in a stochastic manner (Hahn and Malhotra 2000). This could cause diffusion of the spin axis inside the separatrix. If the g_{18} splits into a cluster of similar terms, this could introduce chaos in a manner similar to that found for Mars (Touma and Wisdom 1993; Lascar and Robutel 1993). However, current orbit theory does not yet show much evidence this.

An intriguing alternative is to evoke *two* passes through g_{18} starting with a non-adiabatic passage in the non-capture direction during Saturn's Kelvin-Helmholtz contraction. During contraction, the spin angular momentum of Saturn, $L = \lambda MR^2\omega$, remains constant so that $\omega \propto R^{-2}$. Equation (1) then indicates that α increases with the quantity $J_2 R^2$, while the rotationally induced value of J_2 is $\omega^2 R^3 / GM_s$ (e.g., Kaula 1968). Consequently, $J_2 R^2 \propto \omega^2 R^5 \propto R$, and $\alpha = \alpha_o (R/R_o + q)/(1 + q)$ was larger when Saturn was more distended, where (α_o, R_o) denote the current precession constant and planetary radius. Accordingly, an increase of $\delta R/R_o \geq (1 + q)\delta g/\alpha_o$ would more than compensate for a primordial increase in g_{18} , reinstating Saturn to the right of the resonance in Figure 3. Contraction then drives Saturn through the resonance in the non-capture direction with a maximum induced obliquity of 14.5° . If the passage is fast enough to break the adiabatic invariant at some point, the induced obliquity, $\theta \approx gI\sqrt{2\pi/\dot{\alpha}}$, will be less than the adiabatic value (Appendix). Consequently, the minimum pre-capture obliquity θ_{\min} could be used to put a limit on how fast Saturn could have contracted during its first resonance passage. The minimum characteristic timescale, $\tau \equiv \alpha/|\dot{\alpha}|$, for resonance passage is

$$\tau_{\min} \approx \frac{2\pi}{g_{18}} \left(\frac{\theta_{\min}}{2\pi I_{18}} \right)^2 \approx 2 \times 10^8 \text{ years} \quad (23)$$

which in turn implies a minimum characteristic contraction timescale $\tau_R \equiv R/\dot{R} = \tau_{\min}/(1 + q/J_2) \approx 5 \times 10^7 \text{ years}$. This is consistent with models of the contraction of the gas giant planets using modified stellar evolution codes (e.g., Pollack *et al.* 1976; Bodenheimer and Pollack 1986).

VI. SUMMARY

Saturn's spin axis precession period is close to the precession period (1.87×10^6 years) of the Neptune's orbit plane. We propose that these planets are locked into a secular spin-orbit resonance, and that this is the origin of Saturn's relatively large obliquity (26.7°) compared to that of Jupiter (3.1°). We have outlined a sequence of events that could account

for the establishment of this resonant state. Initially forming with a small obliquity, Saturn passed through the resonance in the capture direction as the Kuiper Belt was depleted, pumping up its obliquity until eventually acquiring its current value. A Saturn currently in resonance places a constraint on that planet's normalized moment of inertia $\lambda > \lambda_{crit} = 0.2233$ and implies the spin axis is librating with an amplitude $\geq 31^\circ$. This could be a fossil remnant of a pre-capture obliquity generated in an earlier resonance pass during the planet's Kelvin-Helmholtz contraction. Alternatively, the librations may have been caused by non-adiabatic conditions during resonance passage (paper II) or excited by a late impact. Numerical experiments described in our companion paper illustrate resonant capture in detail. The critical precession frequency separating circulating from librating spin axis trajectories is $\alpha/g_{18} = -1.18$, $\alpha \cos \theta = 0.730''/yr$, and perhaps further observational data will be able to discriminate between them.

ACKNOWLEDGMENTS

We thank R. Canup, S. Peale, and A. Stern for constructive comments on the manuscript and P. Goldreich for pointing out that a modest impact could excite Saturn's libration about the resonance. WRW was supported by a research grant from NASA's Planetary Geology and Geophysics program. DPH acknowledges support from a NSF career award and from SwRI during his sabbatical stay.

APPENDIX: NON-ADIABATIC OBLIQUITIES

The equation of motion (6) in component form reads

$$\dot{x} = (\alpha z + g \cos I)y - g \sin I z \quad ; \quad \dot{y} = -(\alpha z + g \cos I)x \quad ; \quad \dot{z} = x \sin I \quad (24)$$

Consider again a small angle approximation: $z \sim \cos I \sim 1$, $\sin I \sim I$, and introduce a new independent variable $\varphi \equiv \int_0^t (\alpha + g) dt$, where we take $t = 0$ to be the moment when $\alpha = -g$. The x and y equations can be combined to yield a second order equation $d^2 y / d\varphi^2 + y = gI / (\alpha + g)$ with solution

$$s_y = gI \{-\cos \varphi \int \sin \varphi dt + \sin \varphi \int \cos \varphi dt\} \quad (25)$$

We now expand $\alpha \approx -g + \dot{\alpha}t$ so that $\varphi \approx \dot{\alpha}t^2/2 \equiv t'^2$. Integration of eqn. (22) then gives (Ward *et al.* 1976)

$$y = gI\sqrt{\pi/\dot{\alpha}} \{[C_1(t') + 1/2]\sin t'^2 - [S_1(t') + 1/2]\cos t'^2\} \quad (26)$$

where $C_1(t')$, $S_1(t')$ are Fresnel integrals, and we have required $y \rightarrow 0$ as $t' \rightarrow -\infty$. As $t' \rightarrow +\infty$, C_1 and S_1 approach $1/2$, yielding an obliquity proportional to $\dot{\alpha}^{-1/2}$, viz.,

$$\theta \rightarrow gI\sqrt{2\pi/\dot{\alpha}} \quad (27)$$

REFERENCES

- Agnor, C. B., R. M. Canup and H. F. Levison 1999. *Icarus* **142**, 219
- Allen, C. W. 1976. *Astrophysical Quantities*, London: Athlone (3rd edition).
- Allen, R. L., G. M. Bernstein, and R. Malhotra 2001. *Astrophys. Lett.* **549**, L241
- Applegate, J. H., M. R. Douglas, Y. Gursel, G. J. Sussman, and J. Wisdom, 1986. *Astron. J.* **92**, 176
- Bodenheimer, P., and J. B. Pollack 1986. *Icarus* **67**, 391-408
- Bretagnon, P. 1974. *Astron. Astrophys.* **30**, 141
- Bretagnon and Francou 1992. In *Chaos, Resonances and Collective Dynamical Phenomena in the Solar System* (Ed. S. Ferraz-Mello) Kluwer Academic Publishers, Dordrecht, pp. 37-42.
- Brouwer, D. and G. M. Clemence 1961. *Celestial Mechanics*, Academic Press, New York.
- Brouwer D., and A. J. J. vonWoerkom, 1950. *Astron. Pap. Amer. Ephemeris Nautical Alm.* **12(2)**, 81
- Chambers, J. E. and G. W. Wetherill 1998. *Icarus* **136**, 304
- Columbo, G. 1966. *Astron. J.*, **71**, 891.
- Dones, L. and S. Tremaine 1993. *Icarus* **103**, 67.

- Duncan, M.J., H. F. Levison, and S. M. Budd 1995. *Astron. J.* **110**, 3073
- Farinella, P., D. R. Davis and S. A. Stern 2000. In *Protostars & Planets IV* 2000. (Eds. V. Manning, A. P. Boss and S. S. Russell) Univ. Arizona Press, pp. 1255-1282
- French, R.G., P. D. Nicholson, M. L. Cooke, J. L. Elliot, K. Matthews, O. Perkovic, E. Tollestrup, P. Harvey, N. J. Chanover, M. A. Clark, E. W. Dunham, W. Forrest, J. Harrington, J. Pipher, A. Brahic, I. Grenier, F. Roque, and M. Arndt 1993. *Icarus* **103**, 163.
- Goldreich, P. 1965. *Astron. J.* **70**, 5
- Hahn, J. M. and R. Malhotra 1999. *Astron. J.* **117**, 3041
 _____ 2000. *B.A.A.S.* **32**, 857.
- Hamilton, D. P., and W. R. Ward 2004. *Astron. J.* (*this issue*)
- Harris, A. W. and W. R. Ward, 1982. *Ann. Rev. Earth Planet. Sci.* **10**, 61
- Henrard, J. and C. Murigande 1987. *Celestial Mechanics* **40**, 345.
- Holman, M. J. and J. Wisdom 1993. *Astron. J.* **105**, 1987
- Hubbard, W. B. and M. S. Marley, 1989. *Icarus* **78** 102
- Kaula, W. M. *Introduction to Planetary Physics*, 1968. John Wiley & Sons, Inc., New York.
- Lascar, J. and P. Robutel 1993. *Nature* **361**, 608
- Lissauer, J. J., and V. S. Safronov 1991. *Icarus* **93**, 288.
- Malhotra, R., M. J. Duncan, and H. F. Levison, In *Protostars & Planets IV* 2000. (Eds. V. Manning, A. P. Boss and S. S. Russell) Univ. Arizona Press, pp. 1231-1254
- Nicholson, P. D. and R. G. French 1997. *B.A.A.S.* **29**, 1097.
- Nicholson, P. D., R. G. French and A. S. Bosh 1999. *DPS Abstr.* 31.4402N
- Peale, S. J. 1969. *Astron. J.* **74**, 483
 _____ 1974. *Astron. J.* **79**, 722
- Pollack, J. B., A. S. Grossman, R. Moore and H. C. Graboske 1976. *Icarus* **29**, 35
- Stern, S. A., and J. E. Colwell 1979. *Astron. J.* **114**, 841
- Touma, J. and J. Wisdom 1993. *Science* **259**, 1294
- Tremaine, S. 1991. *Icarus* **89**, 85
- Trujillo, C. A., and M. E. Brown 2001. *Astrophys. Lett.* **554**, L95

- Ward, W. R. 1973. *Science* **181**, 260
- _____ 1974. *J.G.R.* **79**, 3375
- _____ 1975. *Astron. J.*, **80**, 64
- _____ 1979. *J.G.R.* **84**, 237
- _____ 1992. In *Mars*, Eds. H. H. Kieffer, B. M. Jakosky, C. W. Snyder & M. S. Matthews) Univ. Arizona Press: Tucson, AZ, pp. 298-320
- Ward, W. R., G. Colombo and F. A. Franklin 1976. *Icarus*, **28**, 441
- Ward, W. R., J. A. Burns & O. B. Toon 1979. *J.G.R.* **84**, 243.
- Wuchterl, G., T. Guillot and J. J. Lissauer, in *Protostars and Planets IV* 2000. (Eds. V. Mannings, A. P. Boss and S. S. Russell) University of Arizona Press, Tucson, AZ, and reference therein.
- Yoder, C. F. 1995. In *Global Earth Physics: A Handbook of Physical Constants*, AGU Reference Shelf 1 1995.

FIGURE CAPTIONS

Figure 1. Co-precession of orbit normal \mathbf{n} and Cassini state position of spin axis \mathbf{s}_i about the normal \mathbf{k} to the invariable plane.

Figure 2. Spin axis trajectories and Cassini states [shown by vectors \mathbf{s}_1 through \mathbf{s}_4] traced on the unit sphere for a coordinate system rotating about the normal to the invariable plane, \mathbf{k} , with the nodal regression frequency g . The Cartesian coordinate system has its z-axis in the direction of the orbit normal \mathbf{n} and its x-axis along the line of the orbit's ascending node, so that the vector \mathbf{k} lies in the y - z plane, inclined by angle I to \mathbf{n} . The z -coordinate of the spin axis position is the cosine of the obliquity, $z = \cos\theta$. Figure 2b is a polar view of the same unit sphere. The trajectory passing through state 4 is the separatrix (shown bold) that partitions the unit sphere into the three domains. The inclination employed this example to more clearly illustrate the morphology of the trajectories is an order of magnitude larger than the actual $j = 18$ term is used in Figure 4.

Figure 3. Obliquities of Cassini states 1, 2 and 4 as a function of the frequency ratio α/g . Spin axis trajectories circulate about stable states 1 and 2; state 4 is unstable and lies on a separatrix. States 1 and 4 merge and disappear at the critical frequency ratio.

Figure 4. Illustration of the polar view of unit sphere for the $j = 18$ frame of reference for $\alpha/g_{18} = -1.16$. The amplitude of the $j = 18$ terms is $I_{18} = 0.064^\circ$. In addition to the Cassini states, and separatrix, the current spin axis position of Saturn is indicated. The spin axis lies inside the separatrix and circulates state 2 on elongated trajectories that produce libration.

Figure 5. Adiabatic values of the obliquity excited by an arbitrarily slow resonance passage in the non-capture direction as a function of the inclination amplitude, I . The values corresponding to the $j = 16, 17,$ and 18 terms for Saturn's orbit are indicated.

Figure 6. Domain areas as a function of frequency ratio. Top line is sum of domains 1 and 2; second curve is domain 2 only. Lowest curve shows possible loci of area A enclosed by Saturn's current spin axis trajectory. Intersections with A_2 limits the frequency ratio for trapping; intersections with A_{crit} (dotted line) limits the curve to pre-capture obliquities less than 14.5° for which capture is certain.

Figure 7. Capture probabilities into domain 2 as a function of the pre-capture obliquity.

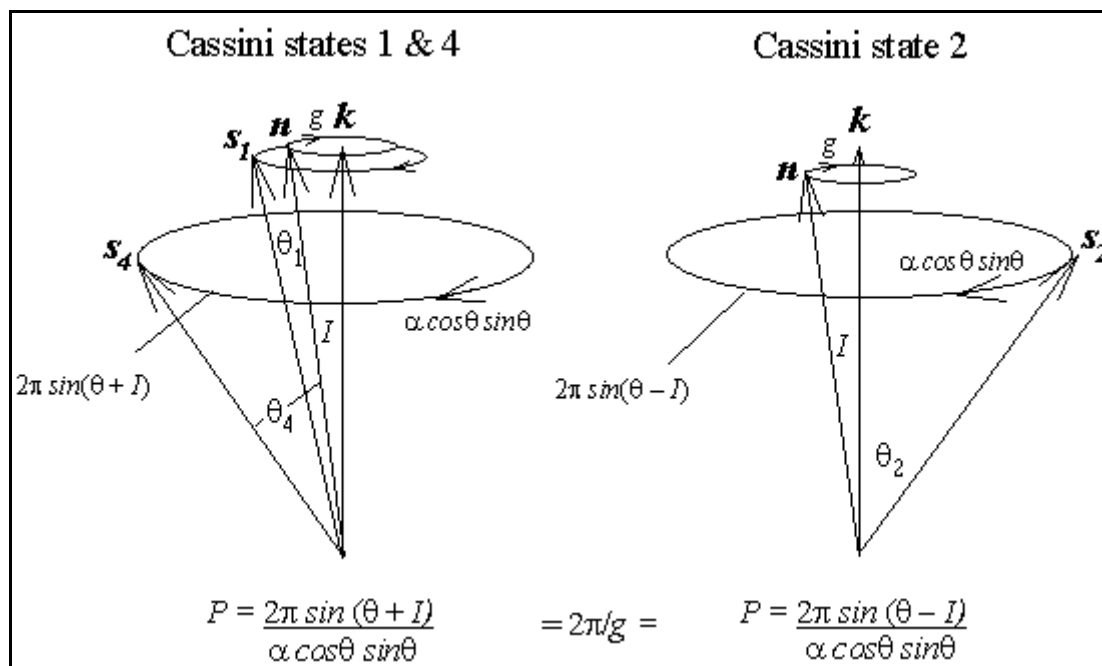


Figure 1

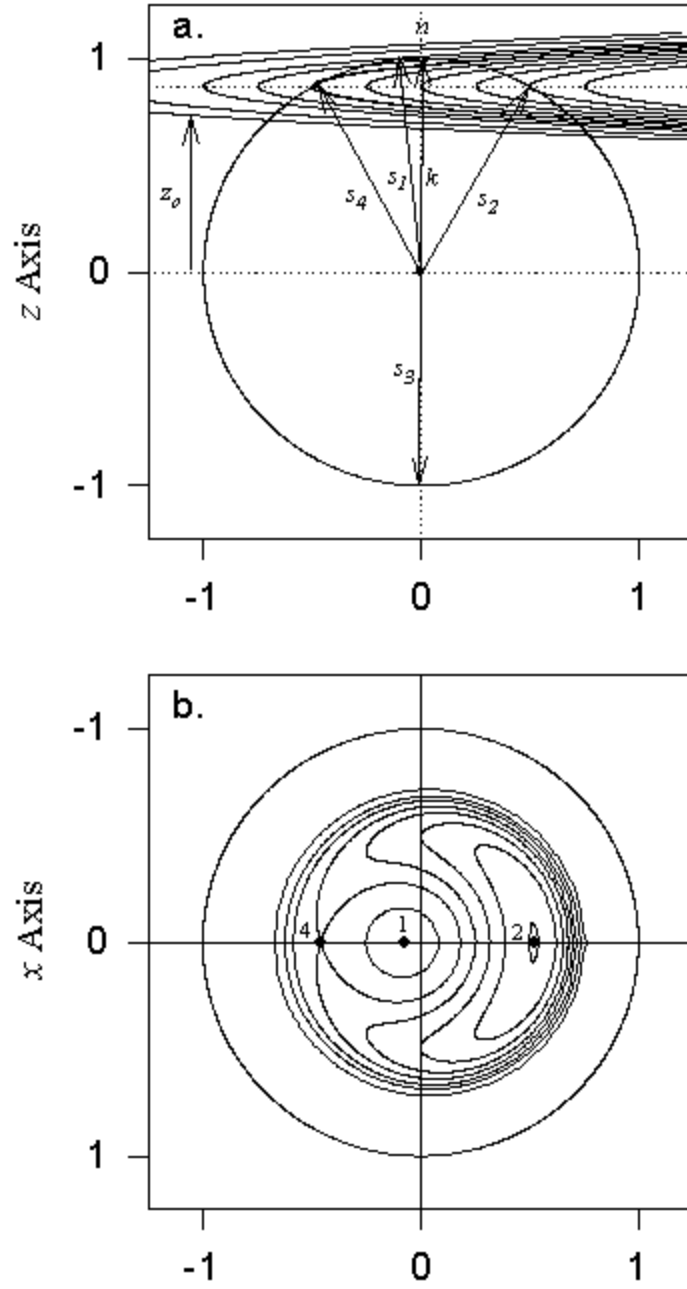


Figure 2

Saturn at the v_{18}

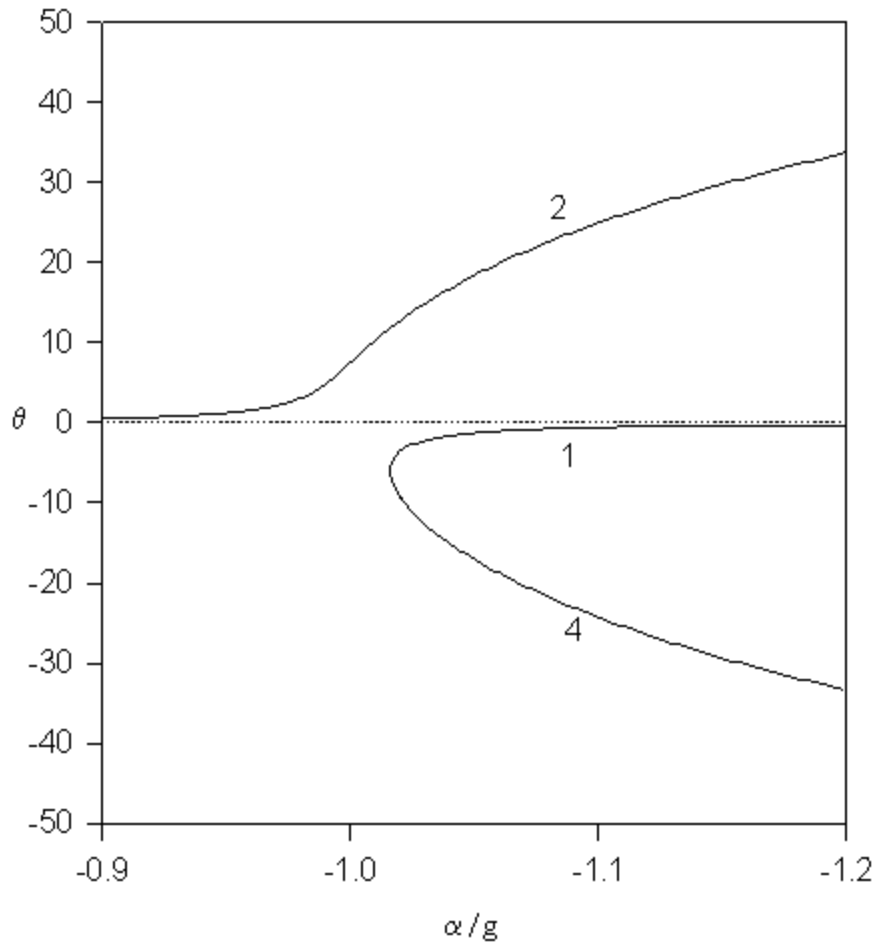


Figure 3.

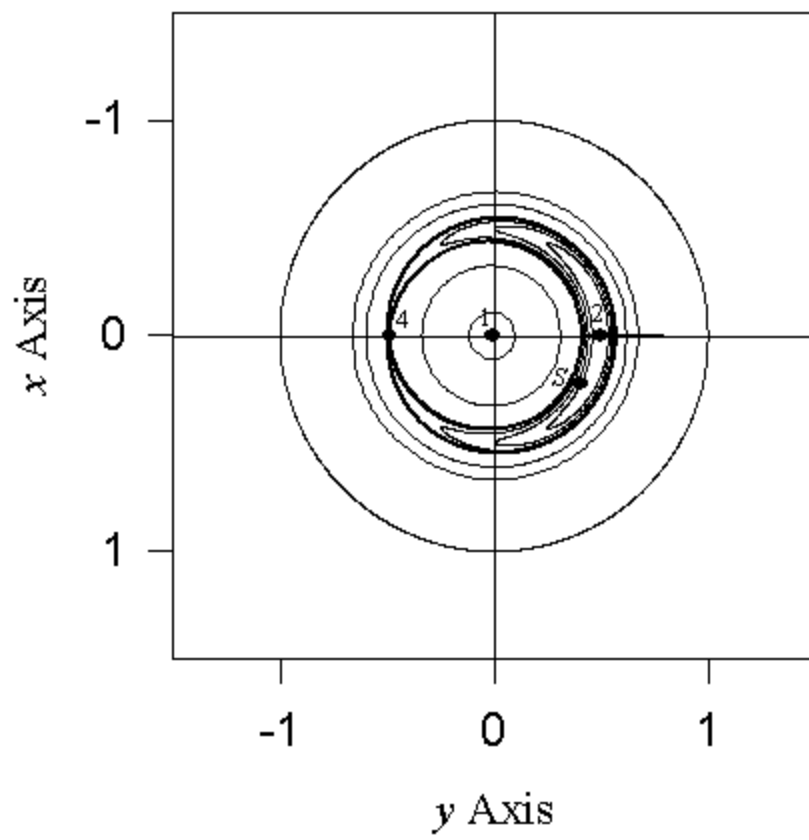


Figure 4

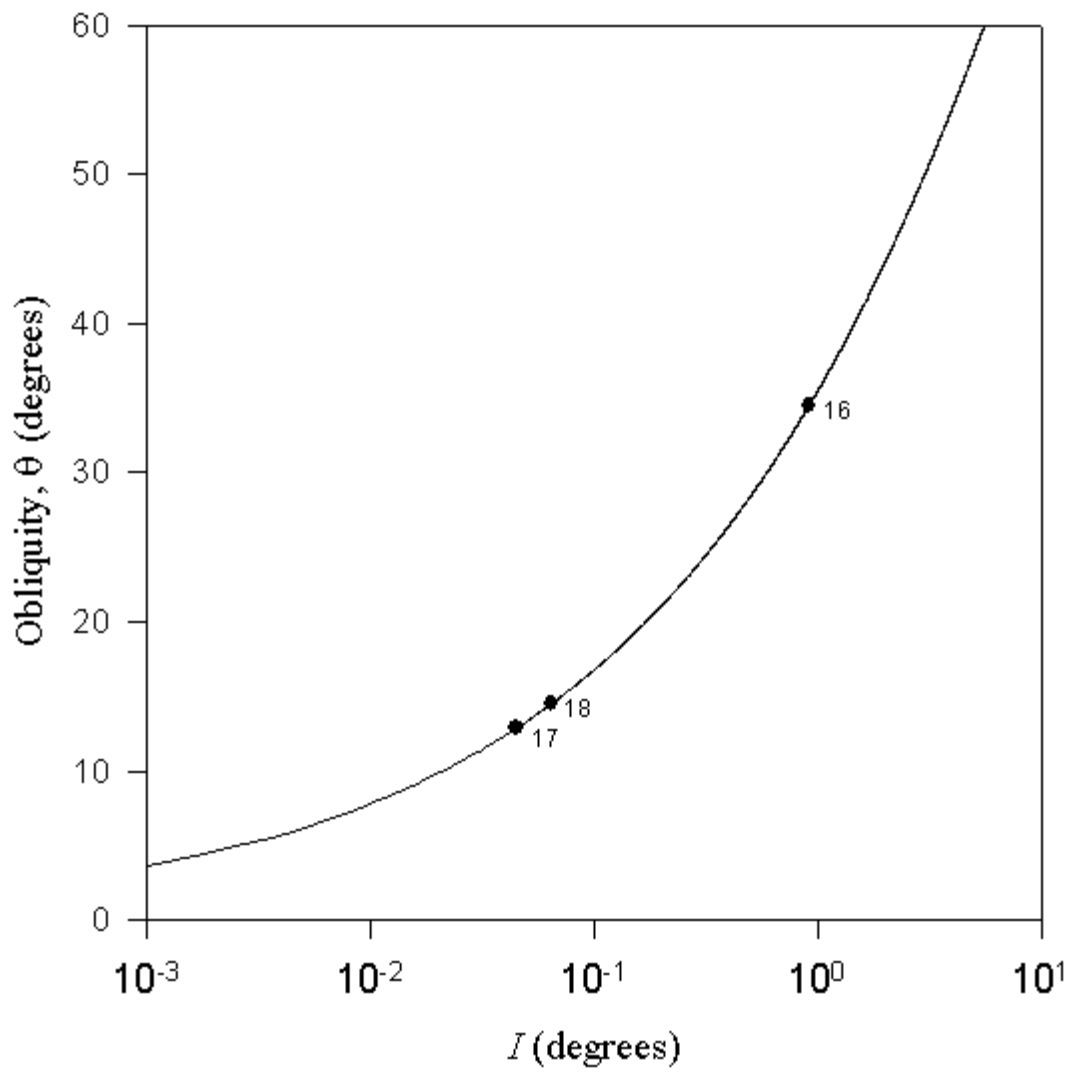


Figure 5

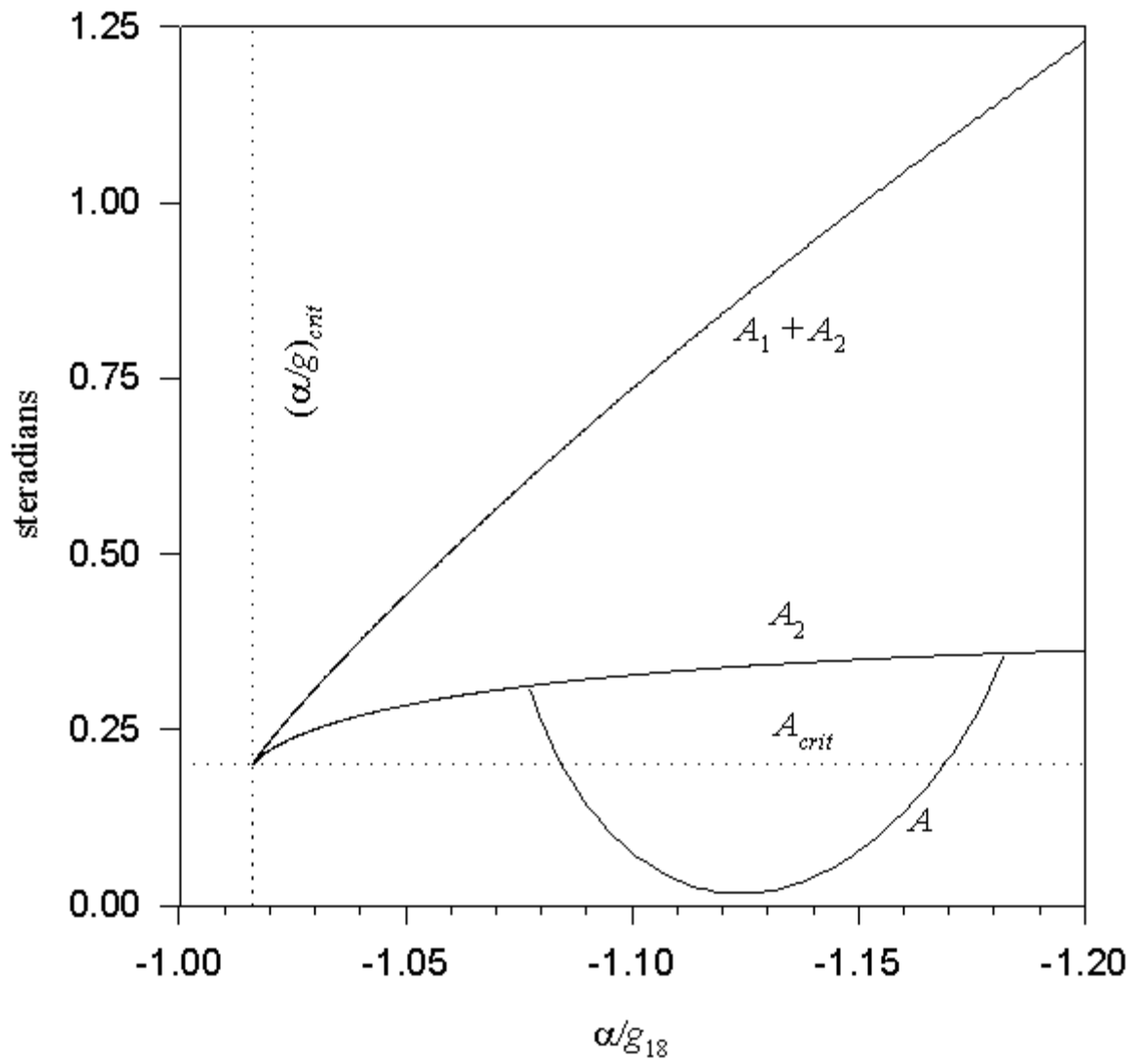


Figure 6

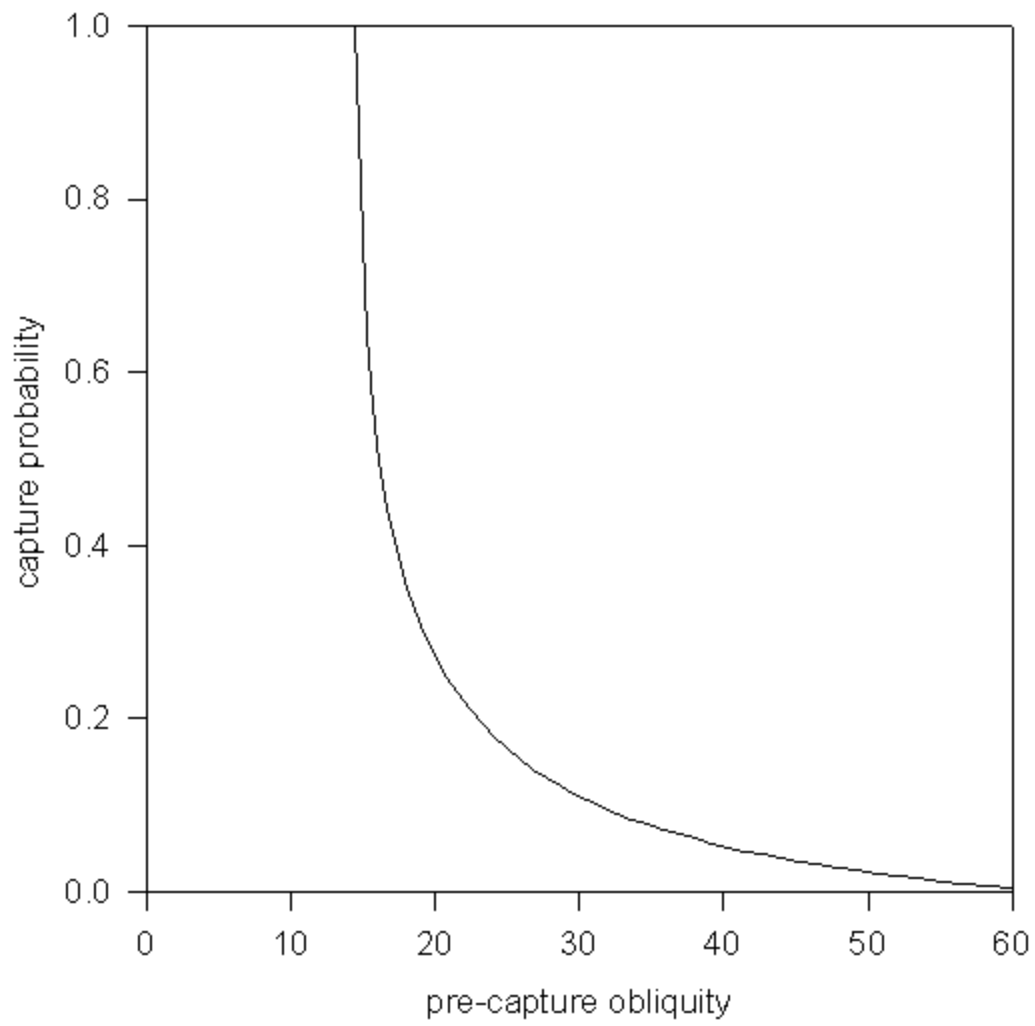


Figure 7